# Structures and electrical conductance of the Si(111)-$\sqrt{3}\times\sqrt{3}$-Ag surface with additional Ag adsorption at low temperatures

Xiao Tong, Shuji Hasegawa, and Shozo Ino
*Department of Physics, School of Science, University of Tokyo, Hongo 7-3-1, Bunkyo-ku, Tokyo 113, Japan*
(Received 3 September 1996)

A phase diagram in the coverage-temperature plane for surface superstructures induced by additional Ag adsorption onto the Si(111)-$\sqrt{3}\times\sqrt{3}$-Ag surface at low temperatures is determined; a $\sqrt{21}\times\sqrt{21}$ phase below 250 K and a $6\times6$ phase below 170 K are formed completely at 0.14 and 0.18 ML, respectively. These structural transformations cause drastic changes in the electrical conductance; the $\sqrt{21}$ phase has much higher conductivity than the initial $\sqrt{3}$ and the 6 phases. The surface migration of Ag adatoms plays an important role in the phenomenon. [S0163-1829(96)08348-8]

The Si(111)-$\sqrt{3}\times\sqrt{3}$-Ag surface is one of the most popular, for which various kinds of surface-science techniques are applied to investigate its atomic arrangement, electronic structure, etc.[1] Although its structure and nature are now clarified, the surface is still an interesting subject in another sense, namely, as a system on which various phenomena occur, contrasting with the clean Si(111)-$7\times7$ surface in many ways. The $\sqrt{3}\times\sqrt{3}$ surface has no dangling bonds, resulting in a semiconductorlike electronic structure and an extreme reduction in surface energy, while the $7\times7$ surface has a metallic surface state due to the dangling bonds. The corrugation on the surface topography of the $\sqrt{3}\times\sqrt{3}$ structure is much smaller than on the $7\times7$ surface. These differences enable comparative studies on phenomena such as atomic-layer growths and the resulting electrical properties.[2,3] In fact, when additional Ag atoms are deposited onto the respective surfaces at room temperature (RT), they are known to grow in quite different styles as revealed through the reflection high-energy electron diffraction (RHEED) and scanning electron microscopy observations;[3] Ag adatoms migrate with extremely high mobility on the $\sqrt{3}\times\sqrt{3}$ surface to make a two-dimensional (2D) gas phase, which nucleate into three-dimensional (3D) islands to leave the $\sqrt{3}\times\sqrt{3}$ surface scarcely covered. The deposited Ag atoms on the $7\times7$ surface, on the other hand, hardly migrate and make flat islands in an incomplete layer-by-layer growth mode. This difference sensitively affects the electrical conduction normal to the surface (through the Schottky barrier[4]) as well as the surface-parallel conduction.[5] The latter electrical conduction of the $\sqrt{3}\times\sqrt{3}$ surface rises steeply with additional Ag adsorption of less than 0.1 ML in a 2D gas phase, while the conductivity decreases when the gas-phase adatoms nucleate into 3D islands.[5,6] At temperatures lower than RT, the surface migration of the deposited Ag adatoms are almost ''frozen'' to suppress the nucleation, and they arrange periodically to make a $\sqrt{21}\times\sqrt{21}$ and a $6\times6$ superstructure.[7]

In the present study, it is found that the adsorption of additional Ag adatoms of only 0.14 ML onto the $\sqrt{3}\times\sqrt{3}$-Ag substrate below 250 K induces a well-ordered $\sqrt{21}\times\sqrt{21}$ superstructure, and exhibits an increase in the surface electrical conductivity. With further deposition up to 0.18 ML below 180 K, the $\sqrt{21}\times\sqrt{21}$ structure transforms into a $6\times6$ phase, which then has a decreasing conductivity. Through the systematic observations both of RHEED and electrical conductance, it is confirmed that the changes in conduction precisely correspond to the transformations of the surface superstructures; only the $\sqrt{21}\times\sqrt{21}$ phase is highly conductive. As far as we know, such structural transformations among well-ordered superstructures and corresponding changes in electrical conduction induced with submonolayer coverages on the low-temperature silicon surface are not reported in the literature. Although further experimental as well as theoretical studies are needed to clarify this correlation between the electrical property and the surface structures, here we especially discuss the extremely high conductivity of the $\sqrt{21}\times\sqrt{21}$ structure in connection with similar $\sqrt{21}\times\sqrt{21}$ structures formed with Au or Cu adsorption onto the $\sqrt{3}\times\sqrt{3}$-Ag surface at RT.

Our UHV chamber had a RHEED system, a sample holder for four-probe conductivity measurements[5] at temperatures ranging from 80 to 1500 K, and an alumina-coated W basket as a Ag evaporator. The substrate was a $p$-type Si(111) wafer of 20 $\Omega$ cm resistivity at RT and its typical dimension was $25\times4\times0.4$ mm$^3$. A clear Si(111)-$7\times7$ RHEED pattern was produced by flashing the sample at 1500 K several times by direct current through it. The $\sqrt{3}\times\sqrt{3}$-Ag surface was prepared by 1 ML Ag deposition with a constant rate of 0.66 ML/min onto the $7\times7$ substrate maintained at 650 K. The deposited amount was monitored with a quartz-crystal oscillator. After this preparation, the sample was cooled down. The temperature of the Si wafer, monitored with an AuFe-Chromel thermocouple attached on the sample holder, could be regulated by pressing the sample holder against the liquid-nitrogen container with controlled force. During Ag deposition under isothermal conditions, the electrical resistance of the wafer was measured as a voltage drop between a pair of Ta wires pressed against the front face of the wafer, with a constant current at 200 $\mu$A flowing through the Ta end clamps.[5] The RHEED beam was turned off during the electrical measurements; the structural changes were observed in separate runs of deposition.

As shown in Figs. 1(a)–1(d), the RHEED patterns successively changed during Ag deposition onto the $\sqrt{3}\times\sqrt{3}$ surface [Fig. 1(a)] at 160 K. The $\sqrt{21}\times\sqrt{21}$ spots began to appear from 0.1 ML coverage, and became the sharpest at 0.14 ML [Fig. 1(b)] corresponding to its saturation coverage. As these spots became weaker after 0.14 ML, the faint

 

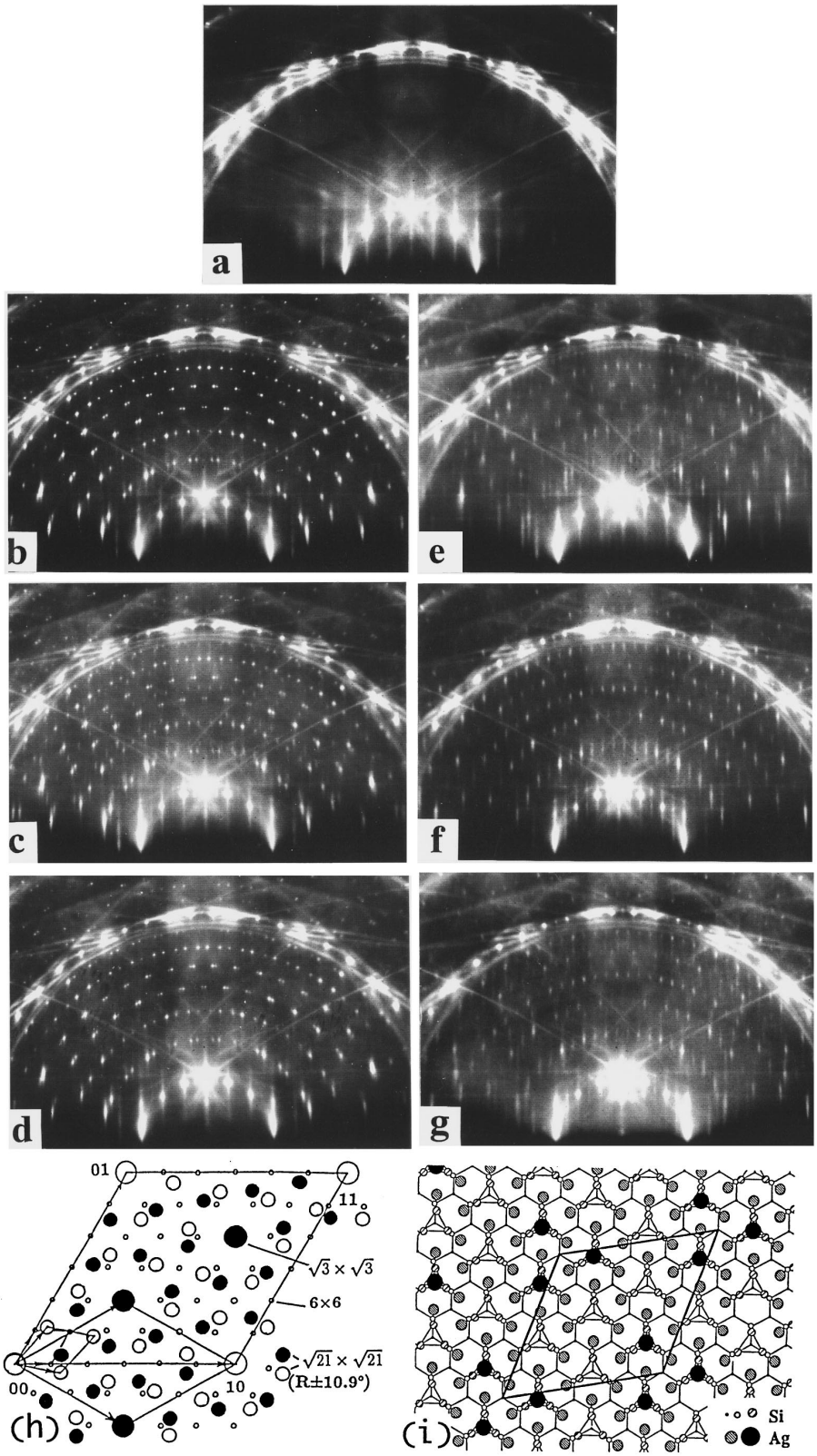


FIG. 1. A series of RHEED patterns taken during additional Ag depositions with a rate of 0.66 ML/min onto the Si(111)-$\sqrt{3}\times\sqrt{3}$-Ag surface (a), at 160 K (b)–(d), and at 100 K (e)–(g), respectively. The additional coverages are (a) 0 ML, (b), (e) 0.1 ML, (c), (f) 0.14 ML, and (d), (g) 0.18 ML, respectively. (b), (d), and (e) the $\sqrt{21}\times\sqrt{21}$ structure, (f) the $6\times6$ structure, and (c), (g) their mixtures. (h) Two-dimensional reciprocal lattices showing the $\sqrt{21}\times\sqrt{21}$ (intermediate solid and open circles for the two equivalent domains), $6\times6$ (small open circles), and the initial $\sqrt{3}\times\sqrt{3}$ (large solid circles) superstructures, respectively. (i) A top view of a structural model for the $\sqrt{21}\times\sqrt{21}$ superstructure. The intermediate shaded circles are Ag atoms composing the $\sqrt{3}\times\sqrt{3}$ framework, while the large solid circles are additional Ag adatoms in an arrangement of the $\sqrt{21}\times\sqrt{21}$ periodicity. This model is based on the one proposed by Ichimiya, Nomura, and Horio (Ref. 8) for the surface on which additional gold adatoms of 0.14 ML are deposited onto the $\sqrt{3}\times\sqrt{3}$-Ag surface at RT.

$6\times6$ spots emerged and became the sharpest at 0.18 ML [Fig. 1(c)] coexisting with the $\sqrt{21}\times\sqrt{21}$ spots. After 0.18 ML the $6\times6$ phase disappeared and only the $\sqrt{21}\times\sqrt{21}$ spots remained, gaining the maximum intensity at 0.30 ML again as shown in Fig. 1(d). Beyond 0.30 ML the $\sqrt{21}\times\sqrt{21}$ spots became weaker to leave only the $\sqrt{3}\times\sqrt{3}$ spots with polycrystalline Ag spots coexisting. At 100 K as shown in Figs. 1(e)–1(g), compared with the corresponding coverages at 160 K, the spots of the $\sqrt{21}\times\sqrt{21}$ structure were weaker and broader at 0.14 and 0.24 ML [Figs. 1(e) and 1(g)] meaning smaller domain sizes. The single phase of the $6\times6$ structure with stronger and sharper spots was observed at 0.18 ML [Fig. 1(f)] at this temperature.

These $\sqrt{21}\times\sqrt{21}$ and $6\times6$ structures disappeared to

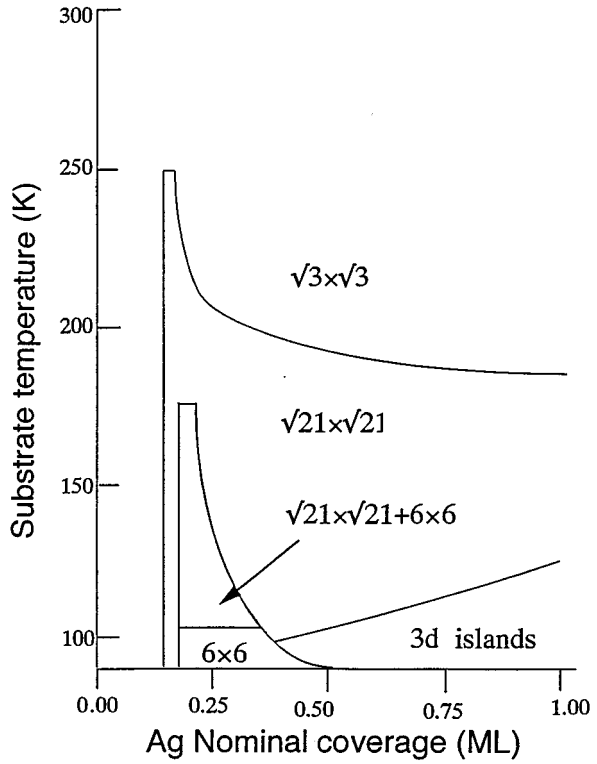


FIG. 2. A phase diagram determined by RHEED observations during Ag deposition with a rate of 0.66 ML/min onto the Si(111)-$\sqrt{3}\times\sqrt{3}$-Ag surface at fixed temperatures. The $(\frac{1}{3},\frac{1}{3})$ spots were always observed in the ranges covered by this diagram.

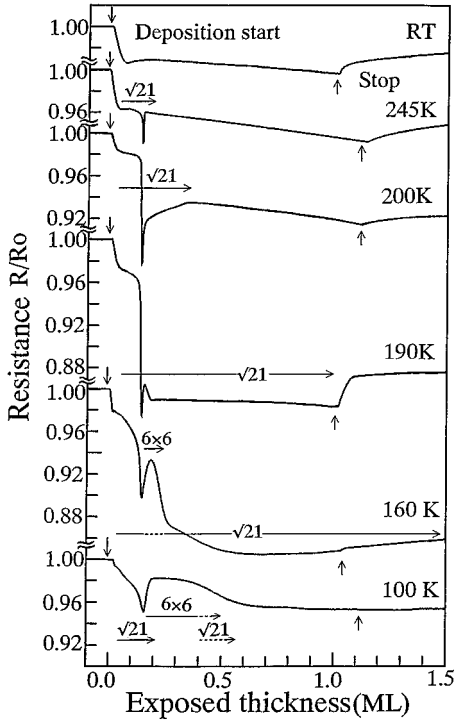


FIG. 3. Changes in the resistance of the Si wafer during Ag depositions with a rate of 0.66 ML/min onto the Si(111)-$\sqrt{3}\times\sqrt{3}$-Ag surface at the respective substrate temperatures. The structural changes observed by RHEED in separate runs of deposition are also indicated.

leave only the $\sqrt{3}\times\sqrt{3}$ spots when the substrate was warmed up to higher than 250 and 180 K, respectively. Figure 2 shows a phase diagram showing the ranges of temperature and Ag coverage in which the respective surface structures were observed. At RT, any structural changes could not be observed by additional Ag deposition; the $\sqrt{3}\times\sqrt{3}$ spots remained strong with coexisting transmission diffraction spots from 3D Ag microcrystals. At 250 K the $\sqrt{21}\times\sqrt{21}$ structure was observed only around 0.14 ML coverage. On cooling from 250 down to 180 K, the intensity of the $\sqrt{21}\times\sqrt{21}$ spots at 0.14 ML increased, and the coverage range for its appearance widened. Below 180 K its intensity became weaker. Below 160 K with more than 0.14 ML coverage, the stable $6\times6$ superlattice spots coexisted with the weak $\sqrt{21}\times\sqrt{21}$ phase, and they became the sharpest at 0.18 ML. Only below 100 K, was the $6\times6$ single phase observed in a restricted range of coverage. A reflection pattern from flat 3D Ag clusters was observed with further depositions.

Figure 3 shows the changes in resistance $R$ (normalized with initial resistance $R_0$) of the wafer during these deposition processes. At RT the resistance steeply dropped by about 3% with less than 0.1 ML coverage, followed by gradual decrease with further deposition. After the evaporator shutter was closed, the resistance rose. These changes are qualitatively similar to the case of an $n$-type Si substrate in previous reports.[2,3,5] At lower temperatures, the initial drop tended to be smaller. Below 250 K, after the initial drop, the resistance slowly decreased with increasing spot intensity of the $\sqrt{21}\times\sqrt{21}$ structure. This corresponds to a stage of the $\sqrt{21}\times\sqrt{21}$ domain growth. Coincident with the maximum intensity of the $\sqrt{21}\times\sqrt{21}$ spots at 0.14 ML, the resistance suddenly dropped. This corresponds to an electrical connection of the growing $\sqrt{21}\times\sqrt{21}$ domains. The amount of the resistance drop at this coverage increased with cooling from 250 to 180 K, up to about 20%, but decreased with further cooling. This means that the areal fraction of the $\sqrt{21}\times\sqrt{21}$ domains at 0.14 ML takes the maximum around 180 K. After 0.14 ML at 245 K, the resistance instantly returned, corresponding to the immediate disappearance of the $\sqrt{21}\times\sqrt{21}$ structure. At 200 K, the rise in resistance beyond 0.14 ML coverage became slow, which corresponded to the process of the gradual disappearance of the $\sqrt{21}\times\sqrt{21}$ structure. At 190 K, the resistance remained almost unchanged beyond 0.14 ML, because the $\sqrt{21}\times\sqrt{21}$ structure continued to exist throughout the deposition. But with the evaporator shutter closed, the resistance rose with the disappearance of the $\sqrt{21}\times\sqrt{21}$ phase. This phenomenon was not observed below 160 K where the $\sqrt{21}\times\sqrt{21}$ phase remained even with the deposition off. At 160 K, the resistance made a temporal small maximum around 0.18 ML in the course of the drop. This process corresponded to the structural transition of the $6\times6$ phase temporarily emerging around 0.18 ML with a mixture of the $\sqrt{21}\times\sqrt{21}$ phase. At 100 K, while the resistance showed a small dip around 0.14 ML corresponding to the short-lived $\sqrt{21}\times\sqrt{21}$ phase, no significant drop in resistance was observed with the appearance of the single-phase $6\times6$ structure.

Figure 4 shows the resistance changes during the sequence of Ag deposition and its interruption at RT [Fig. 4(a)], 180 K [Fig. 4(b)], and 140 K [Fig. 4(c)], respectively. With opening and closing the evaporator shutter, the steep drops and rises in resistance were repeatedly observed in Figs. 4(a) and 4(b). Especially in Fig. 4(b) these changes

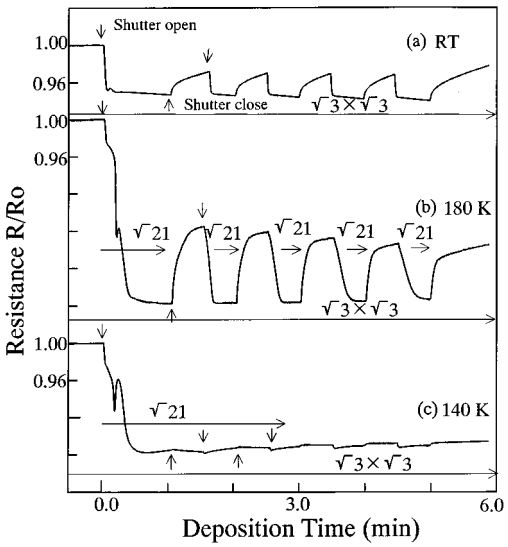


FIG. 4. Changes in the resistance of the Si wafer in the sequence of the Ag deposition with a rate of 0.66 ML/min onto the Si(111)-$\sqrt{3}\times\sqrt{3}$-Ag surface and its interruption at (a) RT, (b) 180 K, and (c) 140 K, respectively. The structural changes are also indicated.

precisely corresponded to the appearance and disappearance of the $\sqrt{21}\times\sqrt{21}$ structure. While no structural changes were observed at RT [Fig. 4(a)], the change in resistance corresponds to the process of surface diffusion and nucleation of Ag adatoms, not due to the radiation from the evaporator;[2,3,5] the adatom density in the 2D gas phase on the surface decreases by being incorporated into 3D Ag islands during the interruption periods, which makes the resistance rise.[6] At 140 K [Fig. 4(c)], the resistance did not rise by stopping the deposition, because the $\sqrt{21}\times\sqrt{21}$ structure remained even during the interruption periods. From these observations, again, it can be said that the $\sqrt{21}\times\sqrt{21}$ phase is highly conductive.

The $\sqrt{21}\times\sqrt{21}$ and $6\times6$ phases appeared only at low temperatures which means that these reconstructions do not involve the destruction of the $\sqrt{3}\times\sqrt{3}$ framework, but are induced just by periodical arrangements of additional Ag adatoms on top of the $\sqrt{3}\times\sqrt{3}$ substrate. The adatoms migrate on the surface with such a high mobility at RT that they cannot be fixed to make superstructures. Even at 180 K as shown in Fig. 4(b), the migration was not completely suppressed, so that the $\sqrt{21}\times\sqrt{21}$ phase could exist only during deposition. The $\sqrt{21}\times\sqrt{21}$ domains at this temperature were formed in the balance of competing processes between the incorporation of Ag adatoms into the $\sqrt{21}\times\sqrt{21}$ domains and their escape from them to nucleate into 3D islands. By switching the deposition off, only the nucleation process proceeded to diminish the $\sqrt{21}\times\sqrt{21}$ domains, resulting in the resistance rise. When the deposition started again, the $\sqrt{21}\times\sqrt{21}$ domains began to grow again on top of the bare $\sqrt{3}\times\sqrt{3}$ framework. Since the surface migration was suppressed enough below 160 K, Ag adatoms constituting the $\sqrt{21}\times\sqrt{21}$ structure scarcely escaped. So the $\sqrt{21}\times\sqrt{21}$ diffraction spots remained unchanged even when the deposition was off [Fig. 4(c)]. By further lowering the temperature, the diffusion length of Ag adatoms on top of the $\sqrt{21}\times\sqrt{21}$ domains also became short enough to form the $6\times6$ structure in turn. At 100 K the diffusion was sufficiently suppressed so that the $6\times6$ domains could grow until the $\sqrt{21}\times\sqrt{21}$ domains were completely converted into the $6\times6$ structure [Fig. 1(f)]. The structural stability of the $\sqrt{21}\times\sqrt{21}$-Ag and $6\times6$-Ag phases thus depends on the surface diffusion of Ag adatoms which is determined by the substrate temperature.

When the $6\times6$ domains are formed, the electronic band structure of the underlying $\sqrt{21}\times\sqrt{21}$ phase totally changes, leading to the resistance increase. When the $6\times6$ domains disappear to recover the $\sqrt{21}\times\sqrt{21}$ structure, the resistance again drops (Fig. 3). The mechanism of the extremely high electrical conductivity of the $\sqrt{21}\times\sqrt{21}$ structure is not clear at present. The surface electrical conductivity on a semiconductor, in general, can be enhanced through the surface space-charge layer, or through the surface-state band, or both. We have additional experimental results indicative of the solution for high conductivity. Similar $\sqrt{21}\times\sqrt{21}$ structures are known to appear by adsorption of Au or Cu of about 0.14 ML on top of the $\sqrt{3}\times\sqrt{3}$-Ag surface at RT.[8,9,10] We have found that these two $\sqrt{21}\times\sqrt{21}$ phases are also highly conductive.[11] By photoemission spectroscopies at RT, furthermore, the $\sqrt{21}\times\sqrt{21}$ phase induced by Au adsorption is found to have a metallic surface-state band crossing over the Fermi level, while the surface space-charge layer tends to be depleted.[11] So the metallic surface-state band is expected to largely contribute to the high conductivity. Since the $\sqrt{21}\times\sqrt{21}$-Ag structure formed at low temperatures dealt with in this paper is very similar to the $\sqrt{21}\times\sqrt{21}$-(Ag+Au) structure at RT as observed by a temperature-variable scanning tunneling microscopy,[12] it is most probable that the same mechanism works for the high conductivity of the $\sqrt{21}\times\sqrt{21}$-Ag surface at low temperature. Further studies by microscopies and spectroscopies at low temperatures are now in progress.

We acknowledge F. Shimokoshi, Dr. T. Takami, Dr. T. Nagao, and Dr. C. S. Jiang for their experimental assistance and stimulating discussions. This work was supported by a Grant-in-Aid from the Ministry of Education, Science and Culture of Japan, and also by the Sumitomo Foundation.

[1] T. Takahashi and S. Nakatani, Surf. Sci. **282**, 17 (1993); Y. G. Ding, C. T. Chan, and K. M. Ho, Phys. Rev. Lett. **67**, 1454 (1991); S. Watanabe, M. Aono, and M. Tsukada, Phys. Rev. B **44**, 8330 (1991).

[2] S. Hasegawa and S. Ino, Int. J. Mod. Phys. B **7**, 3817 (1993).

[3] S. Hasegawa and S. Ino, in *Nanostructures and Quantum Effects*, edited by H. Sakaki and H. Noge (Springer, Berlin, 1994), p. 330.

[4] H. H. Weitering, J. P. Sullivan, R. J. Carolissen, W. R. Graham, and R. T. Tung, Appl. Surf. Sci. **70-71**, 422 (1993).

[5] S. Hasegawa and S. Ino, Phys. Rev. Lett. **68**, 1192 (1992); Surf. Sci. **283**, 438 (1993); Thin Solid Films **228**, 113 (1993).

[6] Y. Nakajima, G. Uchida, T. Nagao, and S. Hasegawa, Phys. Rev. B **54**, 14 134 (1996); A. Natori, M. Murayama, and H. Yasunaga, Surf. Sci. **357–358**, 47 (1996).

[7] Z. H. Zhang, S. Hasegawa, and S. Ino, Phys. Rev. B **52**, 10 760 (1995).

[8] A. Ichimiya, H. Nomura, and Y. Horio, Surf. Rev. Lett. **1**, 1 (1994).

[9] J. Nogami, K. J. Wan, and X. F. Lin, Surf. Sci. **306**, 81 (1994).

[10] I. Homma, Y. Tanishiro, and K. Yagi, in *The Structure of Surfaces III*, edited by S. Y. Tong *et al.* (Springer, Berlin, 1991), p. 610.

[11] C. S. Jiang, S. Hasegawa, and S. Ino, Surf. Sci. (to be published).

[12] X. Tong, Y. Sugiura, T. Nagao, S. Ino, and S. Hasegawa, Surf. Sci. (to be published).